

On the density of states of circular graphene quantum dots

H. Chau Nguyen,^{1,*} Nhung T. T. Nguyen,^{2,3} and V. Lien Nguyen^{2,4}

¹*Max-Planck-Institut für Physik komplexer Systeme,
Nöthnitzer Straße 38, D-01187 Dresden, Germany*

²*Institute of Physics, Vietnam Academy of Science and Technology,
10 Dao Tan, Ba Dinh Distr., 118011 Hanoi, Vietnam*

³*Graduate University of Science and Technology, Vietnam academy of Science and Technology,
18 Hoang Quoc Viet, Cau Giay Distr., 122121 Hanoi, Vietnam*

⁴*Institute for Bio-Medical Physics, 109A Pasteur, 1st Distr., 710115 Hochiminh City, Vietnam*

We suggest a simple approach to calculate the local density of states that effectively applies to any structure created by an axially symmetric potential on a continuous graphene sheet such as circular graphene quantum dots or rings. Calculations performed for the graphene quantum dot studied in a recent scanning tunneling microscopy measurement [Gutierrez *et al. Nat. Phys.* **12**, 1069–1075 (2016)] show an excellent experimental-theoretical agreement.

PACS numbers: 72.80.Vp, 73.63.Kv, 72.10.Fk

Quantum dots are among of the most intensively studied nano-structures. From the application point of view, it is desirable to create quantum dots by feasible and controllable confinement potentials. For conventional semiconductors, such a confinement potential can be easily realized experimentally, e.g., using an appropriate system of gates. The gate-induced electrostatic potentials can be tuned externally to confine electrons to localized states with some desired properties [1]. As for the mono-layer graphene, due to the Klein tunneling, it has been challenging to experimentally realize the potentials that can induce strictly localized electronic states [2, 3]. Fortunately, though electrostatic potentials fail to create truly bound electronic states, they can trap the charge carriers in quasi-bound states (QBSs) with a trapping time long enough to satisfy application requirements [4]. Thus, various confinement potential models have been probed to seek for appropriate QBS-structures [4–11]. Notably, most of the potentials probed [4–11] are axially symmetric, implying that the examined GQDs are circular in shape (circular GQDs - CGQDs).

Each QBS is characterized by its energy and trapping time, expressing respectively as the energy and the width of a resonance emerging in the local density of states (LDOS). One can therefore identify QBSs by analyzing the structure of the LDOS [4]. Alternatively, one can also directly find the energy spectrum of QBSs by solving the Dirac equation with an outgoing wave boundary condition. Generally, the QBS spectrum is then complex: while the real parts give the energy positions of QBSs, the imaginary parts give the inverse of their trapping times [5, 6, 12].

The interest in CGQDs has particularly raised in the recent tunneling spectroscopy measurements [13–16]. It was suggested that the tip of a scanning tunneling microscopy (STM) can be finely adjusted to create a quantum dot on the continuous graphene sheet [13, 14, 16]. It was claimed that all the graphene quantum dots realized in these experiments are practically circular [13, 14, 16]. Impressively, STM is also the tool to detect the LDOS of graphene quantum dots with high precision. In fact, it has been used to explore the electron whispering-gallery mode resonators [13] and to directly image the wave functions of QBSs [13, 15, 16].

To theoretically describe the aforementioned experimental data, one has to calculate the LDOS for the CGQD of interest. In these experiments, the LDOS was calculated either via calculating the scattering coefficients [15] or using the finite difference method [16]. It was claimed in Ref. [15] that the experimental data agree well with the calculated LDOS, except for the QBS of lowest angular momentum. This QBS has made a puzzle by experimentally appearing at the energy considerably higher than theoretically predicted.

In the present work, stimulated by the beautiful STM measurements, we suggest an approach to efficiently calculate the LDOS of any real CGQDs created by an axially symmetric electrostatic potential, avoiding the indirect calculation of scattering coefficients or the computationally expensive finite difference method. As illustrations, we calculate the LDOS in two typical cases of step and smooth confinement potentials. In the former case, the LDOS was calculated for the CGQD measured/calculated in Ref. [15]. Our results describe very well the whole experimental QBS spectrum reported in Ref. [15]. Notably, although not as high as the observed value, our results suggest that the QBS of lowest angular momentum is actually expected to be at higher

* chau@pks.mpg.de

energy than the previous calculation; some part of the puzzle is therefore explained. The factor that makes our approach different from that used in Ref. [15] is clarified. For the studied CGQDs, we also show that the resonance widths (RWs) extracted from our calculated LDOS practically coincide with those obtained from the corresponding complex QBS spectrum of the Dirac equation and qualitatively describe the experimental data. In the case of smooth potentials, we calculate the LDOS for CGQDs created by the Lorentzian shape potential, which is believed to describe the potential induced by a charged STM-tip [9].

For a general CGQD, the Hamiltonian that describes the low energy properties of the trapped electron has the Dirac-Weyl form:

$$\mathcal{H} = \vec{\sigma} \cdot \vec{p} + U(r), \quad (1)$$

where $\vec{\sigma} = (\sigma_x, \sigma_y)$ are Pauli matrices, $\vec{p} = -i(\partial_x, \partial_y)$ is the 2-dimensional momentum operator, and $U(r)$ is an axially symmetric potential. We deal with the case of experiments [13–16] when the valley scattering can be neglected and use units such that $\hbar = 1$ and the Fermi velocity $v_F = 1$.

To calculate the LDOS for the studied CGQDs, one has to solve the eigenvalue equation of Hamiltonian (1) with a proper normalization. Suppose E and $\Psi^{(E)}(r, \phi)$ are the associated eigenvalue and eigenfunction of this Hamiltonian. Since the potential $U(r)$ is axially symmetric, the eigenfunction $\Psi^{(E)}(r, \phi)$ can be found in the form

$$\Psi^{(E,j)}(r, \phi) = e^{ij\phi} \begin{pmatrix} e^{-i\phi/2} \chi_A^{(E,j)}(r) \\ e^{+i\phi/2} \chi_B^{(E,j)}(r) \end{pmatrix}, \quad (2)$$

where the total angular momentum j takes half-integer values and $\chi_{A/B}^{(E,j)}(r)$ are the radial wave functions on the graphene A/B -sublattices. In the following, the dependence of these wave functions on the parameters (E, j) will be made implicit to simplify the notation. The radial wave function $\chi(r) = (\chi_A(r), \chi_B(r))^T$ follows the equation

$$i \frac{\partial \chi(r)}{\partial r} = \mathcal{H}(r) \chi(r), \quad (3)$$

where the formal radial Hamiltonian $\mathcal{H}(r)$ is defined by

$$\mathcal{H}(r) = \begin{pmatrix} i \frac{j-1/2}{r} & U(r) - E \\ U(r) - E & -i \frac{j+1/2}{r} \end{pmatrix}. \quad (4)$$

Certainly, because of the circular symmetry of the structure, the LDOS also depends only on the radial coordinate r and can be found as

$$\rho(E, r) = \sum_{j=-\infty}^{+\infty} \rho^{(j)}(E, r), \quad (5)$$

with

$$\rho^{(j)}(E, r) \propto \frac{1}{\Delta E} \|\chi(r)\|^2, \quad (6)$$

where ΔE is the level spacing at the energy E and $\chi(r)$ has to be subjected to a proper normalization condition. To find the level spacing ΔE and the normalization condition for $\chi(r)$, we follow the approach suggested in Ref. [4]. In this approach, the quantum dot is assumed to be embedded in a large graphene disk of radius R . The disk is so large that for much of its area, the potential $U(r)$ is practically flat. In this case, one can assume there exists some distance $r_f \ll R$ such that for $r \geq r_f$, the potential could be considered constant, $U(r) \equiv U_f$. Consequently, for $r \geq r_f$, the wave function can be expressed in terms of two integral constants $C_f = (C_f^{(1)}, C_f^{(2)})^T$:

$$\chi(r) = W_f(r) C_f, \quad (7)$$

where

$$W_f(r) = \begin{pmatrix} J_{j-\frac{1}{2}}(q_f r) & Y_{j-\frac{1}{2}}(q_f r) \\ i\tau_f J_{j+\frac{1}{2}}(q_f r) & i\tau_f Y_{j+\frac{1}{2}}(q_f r) \end{pmatrix}, \quad (8)$$

with $q_f = |E - U_f|$ and $\tau_f = \text{sign}(E - U_f)$. The two columns of this $W_f(r)$ -matrix are just the two independent basic solutions to the Hamiltonian $\mathcal{H}(r)$ in the region considered (see [17] for the details). Then, using the fact that the wave function vanishes at $r = R$, one finds the level spacing to be [4]

$$\Delta E = \frac{\pi}{R}. \quad (9)$$

Next, the normalization condition for the wave function can be found by requiring that the integration of the electronic probability density over the whole disk must be 1. Since for much of the disk area, the wave function is of the form (8), one can simply ignore the area inside the quantum dot from this integration [4]. This ultimately results in the following normalization condition [4]:

$$\frac{4R \|C_f\|^2}{|E - U_f|} = 1. \quad (10)$$

The problem that is left is to find an appropriate initial condition so that the differential eq. (3) can be solved. The case when the potential can be considered to be flat near the origin, namely, $U(r) = U_i$ for $r \leq r_i$, has been studied using the T -matrix method [17]. In this case the eigenfunction of eq. (3) near the origin has the simple form

$$\chi(r) = \mathcal{N} \begin{pmatrix} J_{j-\frac{1}{2}}(q_i r) \\ i\tau_i J_{j+\frac{1}{2}}(q_i r) \end{pmatrix}, \quad (11)$$

with $q_i = |E - U_i|$, $\tau_i = \text{sign}(E - U_i)$ and \mathcal{N} being the normalization coefficient. One then can just take the solution (11) at r_i as the initial values and solve eq. (3) for $\chi(r)$. The normalization coefficient is found by imposing

the condition (10), where C_f is related to $\chi(r_f)$ by eq. (7). With the wave function normalized, the LDOS can be now calculated using equations (5) and (6).

Though the assumption that the radial potential $U(r)$ is flat near the origin ($r < r_i$) is really observed in different CGQD-models [4, 6–8, 15], with regard to the confinement potentials induced by the STM-tip in experiments reported in Ref. [13, 14, 16], there is a need to relax this assumption. Note that, on the other hand, the similar assumption of the flatness of the potential in the opposite limit of large distances ($r > r_f$) is naturally met for all the realistic CGQDs created by a short range electrostatic potential.

When the potential $U(r)$ is not flat, the wave function (11) is no longer an exact solution of eq. (3). However, if $U(r)$ is continuous and bounded near the origin, the asymptotic form of (11) still correctly describes the asymptotic behavior of the solution, namely $\chi(r) \sim (\propto r^{|j-\frac{1}{2}|}, \propto r^{|j+\frac{1}{2}|})$ [Here, to avoid irrelevant factors we use the symbols \propto]. However, except for $j = \pm\frac{1}{2}$, this asymptotic solution vanishes at the origin ($r = 0$), thus cannot be used as the initial value to solve the differential eq. (3) for $\chi(r)$. The simple trick to get around this problem is to consider the regularized wave function $\tilde{\chi}(r) = r^{-\beta}\chi(r)$, where $\beta = \min\{|j-\frac{1}{2}|, |j+\frac{1}{2}|\}$. The modified wave function $\tilde{\chi}(r)$ follows the evolution

$$i\frac{\partial\tilde{\chi}}{\partial r} = \tilde{\mathcal{H}}(r)\tilde{\chi}(r) \quad (12)$$

with

$$\tilde{\mathcal{H}}(r) = \mathcal{H}(r) - \frac{i\beta}{r}. \quad (13)$$

The initial condition for the regularized wave function $\tilde{\chi}(r)$ is now regular, namely, $\tilde{\chi}(0) = (\tilde{\mathcal{N}}, 0)^t$ if $|j-\frac{1}{2}| < |j+\frac{1}{2}|$ and $\tilde{\chi}(0) = (0, \tilde{\mathcal{N}})^t$ otherwise. Here $\tilde{\mathcal{N}}$ is the normalization coefficient, which is found using (7) and (10) as described above. With the wave function determined from $\tilde{\chi}(r)$, the LDOS can again be calculated using (5) and (6).

As a typical illustration for the suggested approach, we calculate the LDOS for the CGQD studied in Ref. [15]. This CGQD is believed to exhibit a sharp boundary so that the radial confinement potential can be modeled as a step one, $U(r) = V_0\Theta(R-r)$, where $V_0 = \text{constant}$, $\Theta(x)$ is the Heaviside step function, and R is the dot radius. The LDOS can then be calculated from eqs. (5) and (6) with the wave function $\chi(r)$ determined directly from eq. (3). Note that without an external magnetic field, the energy spectra are identical for $j > 0$ and $j < 0$ [5, 6], we therefore consider only the case $j > 0$.

Fig. 1 compares (a) the experimental data provided by the authors of Ref. [15] and (b) our calculated LDOS. Both figures were plotted in the same format, giving a clear view of the full spectrum through a cross-sectional slice of the CGQD. The corresponding experimental and theoretical total density of states (TDOS) are calculated and presented in Fig.1c by the dashed and solid lines,

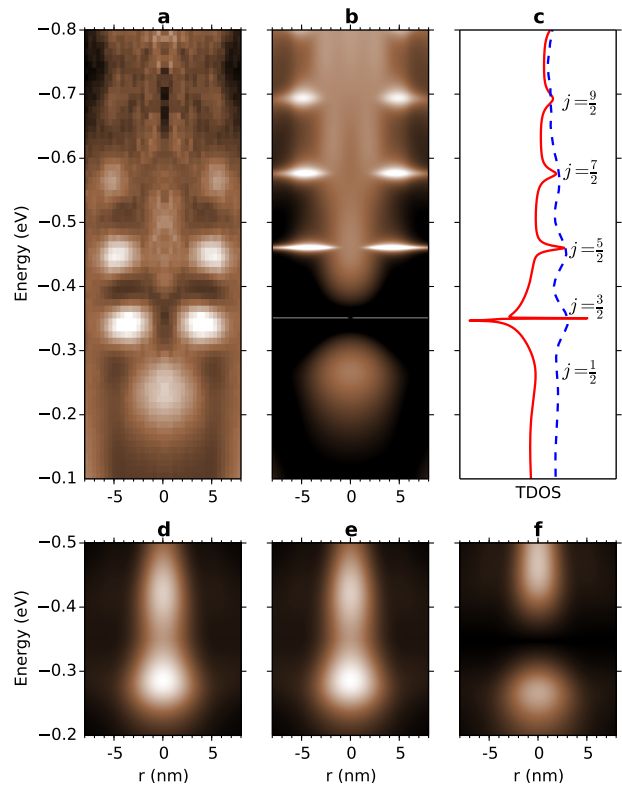


FIG. 1. (a, b) LDOSs of CGQD with $R = 5.93$ nm, $V_0 = 0.43$ eV (corrected background $E_D = -0.347$ eV. [15]): (a) Experimental data provided by the authors of Ref. [15]; (b) Calculated results using the present approach; (c) Two TDOSs calculated from the data in (a) (dashed) and (b) (solid line) [log scale, arbitrary unit]. The resonances are labeled by their angular momentum. Panels (d – f) compare the partial LDOSs for the state of $j = \frac{1}{2}$: (d) from Ref. [15]; (e) Eq. (6) without normalization; (f) Eq. (6) with normalization.

respectively. The resonances observed in Fig. 1c are labeled by their angular momentum j . Obviously, on the whole, there is a very good agreement between the experimental data and our theoretical calculation. Particularly, our calculation gives a better agreement for the state of lowest angular momentum $j = \frac{1}{2}$, compared to the calculation reported in Ref. [15]. A closer analysis shows that the difference between the two calculated results mainly stems from the normalization eq. (10). This normalization was absent from the scattering calculations in Ref. [15], but naturally appears in the direct calculation described above. As a particular verification of this intuitive assessment, we compare the partial LDOSs for just the state of $j = \frac{1}{2}$ calculated: from the scattering approach in Ref. [15] (Fig. 1d); from eq. (6) discarding the normalization (10) (Fig. 1e); and from eq. (6) with the normalization (10) (Fig. 1f). Obviously, while the two figures Fig. 1d and Fig. 1e are practically identical, the normalization pushes the state in Fig. 1f closer to the experimental position. It should be noted that, despite this improvement, a small discrepancy between the

theoretical prediction and the experimental position of this state persists. We speculate that, having the largest level width, the $j = \frac{1}{2}$ state is more susceptible to various fluctuations such as the imperfection of the dot boundary (as suggested in Ref. [15]) or the thermal noise, which further affect its position.

Although the experimental and theoretical TDOS-lines in Fig. 1c show the resonances at almost the same energies, we also notice that the theoretical widths are noticeably smaller than experimental ones. To assess this experimental-theoretical discrepancy, we determine the widths of the resonances in Fig. 1c by fitting the TDOS around each resonance to a Lorentzian peak [4, 15]. The resonance of $j = \frac{9}{2}$ is excluded due to the low quality of the experimental data. For the rest, the widths obtained from the two TDOSs are compared in Fig. 2. It seems that for all the resonances examined, the experimental widths (vertical axis) are in the same amount of ≈ 0.028 eV larger than the theoretical ones (horizontal axis). This systematic smearing of resonances (that makes peaks wider and lower) may be caused by, as was already noted in Ref. [15], the fact that the electrons in graphene have a non-zero probability of transition into the surface of the copper substrate, which leads to a decrease of the trapping times in QBSs. The thermal noise might be an additional reason for this resonance smearing.

For the same QBSs of $j = \frac{1}{2}, \frac{3}{2}, \frac{5}{2},$ and $\frac{7}{2}$ of the studied CGQD, we also calculate the imaginary parts $\text{Im} E$ of the QBS complex energies E using our T -matrix approach suggested in Ref. [17]. For a given QBS, this imaginary part of the energy should provide a direct measure of the resonance width. In the inset in Fig. 2, we show the obtained $(-\text{Im} E)$ in comparison with the resonance widths extracted from the calculated TDOS. We find that for all the resonances examined, the resonance widths extracted from TDOS (horizontal axis) and the corresponding imaginary parts of the QBS complex energies (vertical axis) practically coincide. This gives additional confidence to the current discussion.

As another illustration, we calculate the LDOS for the CGQDs of the type that is created by a charged STM-tip in the experiments reported in Refs. [13, 16]. We follow Ref. [9] and model these smooth potentials as: $U(r) = V_0/[1 + (r/R_0)^2]$ (Lorentzian potentials), where V_0 and R_0 measure the strength and the width of the potential, respectively. Although the LDOS can still be calculated from eqs. (5) and (6), since the potential is not flat in the vicinity of the origin, the wave function $\chi(r)$ in these equations should be determined from the regularized one $\tilde{\chi}(r)$ of eq. (12). In fact, this approach is very general in the sense that it can be effectively applied to calculate the LDOS of any realistic CGQD created by electrostatic potentials. We show in Fig. 3 the LDOS (a) and the corresponding TDOS (b) calculated for the CGQD with the Lorentzian confinement potential of $R_0 = 50$ nm and $V_0 = 0.15$ eV. Certainly, from this figure, we can extract the resonance widths in the same way as presented above.

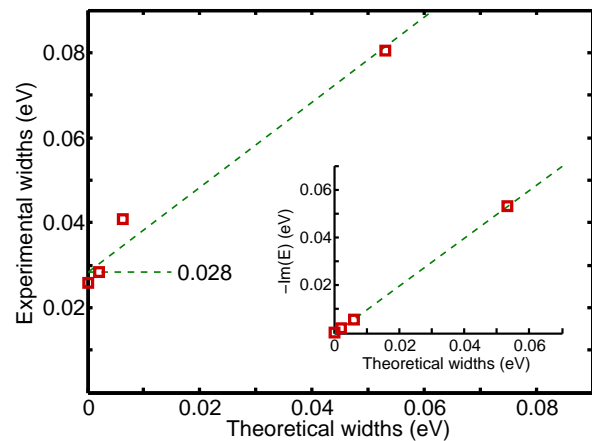


FIG. 2. Resonance widths of the QBSs of $j = \frac{1}{2}, \frac{3}{2}, \frac{5}{2},$ and $\frac{7}{2}$ (indicated in Fig.1c). Main figure: Experimental-theoretical comparison of the widths extracted from the two TDOSs in Fig. 1(c). The dashed straight-line has unity slop and a fitted offset of 0.028eV. Inset: the widths extracted from calculated TDOS and $-\text{Im} E$ are in comparison. The dashed straight-line has unity slop and zero offset.

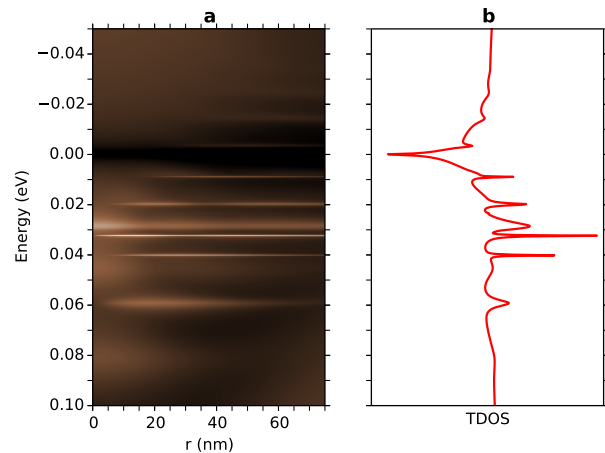


FIG. 3. LDOS (a) and TDOS (b) for the CGQD created by the Lorentzian potential with $V_0 = 0.15$ eV and $R_0 = 50$ nm.

Owing to the lack of detailed experimental data available for comparison, we would like simply to note the rather dense and narrow resonances emerged in the figure. The whole spectrum is also very sensitive to both parameters V_0 and R_0 .

Thus we have presented an approach to calculate the LDOS of CGQDs. This approach equally applies to practically any structure created by axially symmetric electrostatic potentials on a continuous graphene sheet. It can in principle be extended to the cases when a mass term and/or an external perpendicular magnetic field are added to the Hamiltonian (1). In these cases, however, the valley splitting should also be taken into account.

ACKNOWLEDGMENTS

We would like to thank Abhay Narayan Pasupathy and Christopher Gutierrez for sharing their excellent exper-

imental data and for helpful discussions. This research is funded by Vietnam National Foundation for Science and Technology Development (NAFOSTED) under grant number 103.02-2015.48

-
- [1] T. Chakraborty, *Quantum Dots: A survey of the properties of artificial atoms* (Elsevier, 1999).
- [2] M. I. Katsnelson, K. S. Novoselov, and A. K. Geim, “Chiral tunnelling and the Klein paradox in graphene,” *Nat. Phys.* **2**, 620–625 (2006).
- [3] A. H. C. Neto, F. Guinea, N. M. R. Peres, K. S. Novoselov, and A. K. Geim, “The electronic properties of graphene,” *Rev. Mod. Phys.* **81**, 109 (2009).
- [4] A. Matulis and F. M. Peeters, “Quasibound states of quantum dots in single and bilayer graphene,” *Phys. Rev. B* **77**, 115423 (2008).
- [5] H.-Y. Chen, V. Apalkov, and T. Chakraborty, “Fock-Darwin states of Dirac electrons in graphene-based artificial atoms,” *Phys. Rev. Lett.* **98**, 186803 (2007).
- [6] P. Hewageegana and V. Apalkov, “Electron localization in graphene quantum dots,” *Phys. Rev. B* **77**, 245426 (2008).
- [7] P. Recher, J. Nilsson, G. Burkard, and B. Trauzettel, “Bound states and magnetic field induced valley splitting in gate-tunable graphene quantum dots,” *Phys. Rev. B* **79**, 085407 (2009).
- [8] J. H. Bardarson, M. Titov, and P. W. Brouwer, “Electrostatic confinement of electrons in an integrable graphene quantum dot,” *Phys. Rev. Lett.* **102**, 226803 (2009).
- [9] C. A. Downing, D. A. Stone, and M. E. Portnoi, “Zero-energy states in graphene quantum dots and rings,” *Phys. Rev. B* **84**, 155437 (2011).
- [10] M. Schneider and P. W. Brouwer, “Density of states as a probe of electrostatic confinement in graphene,” *Phys. Rev. B* **89**, 205437 (2014).
- [11] J.-S. Wu and M. M. Fogler, “Scattering of two-dimensional massless Dirac electrons by a circular potential barrier,” *Phys. Rev. B* **90**, 235402 (2014).
- [12] H. C. Nguyen, M. T. Hoang, and V. L. Nguyen, “Quasibound states induced by one-dimensional potentials in graphene,” *Phys. Rev. B* **79**, 035411 (2009).
- [13] Y. Zhao, J. Wyrick, F. D. Natterer, J. F. Rodriguez-Nieva, C. Lewandowski, K. Watanabe, T. Taniguchi, L. S. Levitov, N. B. Zhitenev, and J. A. Stroscio, “Creating and probing electron whispering-gallery modes in graphene,” *Science* **348**, 672–675 (2015).
- [14] N. M. Freitag, L. A. Chizhova, P. Nemes-Incze, C. R. Woods, R. V. Gorbachev, Y. Cao, A. K. Geim, K. S. Novoselov, J. Burgdörfer, F. Libisch, and M. Morgenstern, “Electrostatically confined monolayer graphene quantum dots with orbital and valley splittings,” *Nano Lett.* **16**, 5798 (2016).
- [15] C. Gutiérrez, L. Brown, C.-J. Kim, J. Park, and A. N. Pasupathy, “Klein tunnelling and electron trapping in nanometre-scale graphene quantum dots,” *Nat. Phys.* **12**, 1069–1075 (2016).
- [16] J. Lee, D. Wong, J. Velasco Jr, J. F. Rodriguez-Nieva, S. Kahn, H.-Z. Tsai, T. Taniguchi, K. Watanabe, A. Zettl, F. Wang, L. S. Levitov, and M. F. Crommie, “Imaging electrostatically confined Dirac fermions in graphene quantum dots,” *Nat. Phys.* , 1032–1036 (2016).
- [17] H. C. Nguyen, Nhung T. T. Nguyen, and V. L. Nguyen, “The transfer matrix approach to circular graphene quantum dots,” *J. Phys.: Condens. Matt.* **28**, 275301 (2016).